Published in final edited form as:
*Development*. 2008 May ; 135(9): 1615–1624. doi:10.1242/dev.012179.

# Requirement for Foxd3 in Maintenance of Neural Crest Progenitors

**Lu Teng**[2,1,6], **Nathan A. Mundell**[4,5,1], **Audrey Y. Frist**[3,5], **Qiaohong Wang**[2], and **Patricia A. Labosky**[2,3,4,5,*]

2 *Department of Cell and Developmental Biology, University of Pennsylvania School of Medicine, Philadelphia, PA 19104-6058, USA*

3 *Department of Cell and Developmental Biology, Vanderbilt University School of Medicine, Nashville, TN 37232-0494, USA*

4 *Department of Pharmacology, Vanderbilt University School of Medicine, Nashville, TN 37232-0494, USA*

5 *Center for Stem Cell Biology, Vanderbilt University School of Medicine, Nashville, TN 37232-0494, USA*

## Summary

Understanding the molecular mechanisms of stem cell maintenance is critical for the ultimate goal of manipulating stem cells for treatment of disease. Foxd3 is required early in mouse embryogenesis; *Foxd3*$^{-/-}$ embryos fail around the time of implantation, cells of the inner cell mass cannot be maintained *in vitro*, and blastocyst-derived stem cell lines cannot be established. Here, we report that Foxd3 is required for maintenance of the multipotent mammalian neural crest. Using tissue specific deletion of *Foxd3* in the neural crest, we show that *Foxd3*$^{flox/-}$; *Wnt1-Cre* mice die perinatally with a catastrophic loss of neural crest-derived structures. Cranial neural crest tissues are either missing or severely reduced in size, the peripheral nervous system consists of reduced dorsal root ganglia and cranial nerves, and the entire gastrointestinal tract is devoid of neural crest derivatives. These results demonstrate a global role for this transcriptional repressor in all aspects of neural crest maintenance along the anterior-posterior axis, and establish an unprecedented molecular link between multiple divergent progenitor lineages of the mammalian embryo.

### Keywords

Neural crest; Foxd3; mouse embryo; stem cell maintenance

## Introduction

The neural crest (NC) are multipotent progenitor cells possessing the unique ability to contribute to a variety of disparate adult derivatives: the entire peripheral and enteric nervous systems (PNS and ENS), bones and connective tissue of the head and neck, and the outflow tract of the developing heart among others. NC cells emigrate from the dorsal neural tube during early embryogenesis and migrate to final sites of differentiation. Their fate depends on their rostral-caudal position of origin in the neural tube, their route of migration and final destination (reviewed in Le Douarin and Kalcheim, 1999). Many of the cellular mechanisms critical to development of an embryo are represented within this extraordinary tissue: specification of

* Author for correspondence, trish.labosky@vanderbilt.edu, Phone 615-322-2540, Fax 615-322-6645.
[1]These authors contributed equally to this work.
[6]Present address: Children's National Medical Center, Washington DC 20010-2970.

cell type, maintenance of multipotency of progenitor cells, directed migration of cells to their final destination and terminal differentiation of cells. Members of the PDGF, BMP and Wnt families of secreted molecules are important for the initial specification and subsequent maintenance of the NC (reviewed in (Steventon et al., 2005). And many transcription factors are activated in NC in response to these signaling cascades. These include Foxd3, Sox8, 9 and 10 (Cheung and Briscoe, 2003); (Southard-Smith et al., 1998), Ap2 (Schorle et al., 1996), Pax3 (Epstein et al., 1991), and others. It is not yet clear how these factors work together to induce and then maintain this unique cell type.

The *Foxd3* gene encodes a transcriptional repressor of the winged helix or "Forkhead" family of proteins (Labosky and Kaestner, 1998; Sutton et al., 1996). This large family of proteins is characterized by a 100 amino acid DNA-binding domain and transcriptional activation or repression domains (reviewed in Labosky and Kaestner, 2005; Wijchers et al., 2006). *Foxd3* was first characterized by its expression in embryonic stem cells (ES cells) and multipotent cells of the NC (Labosky and Kaestner, 1998). Our previous work demonstrated that Foxd3 is required early in mouse embryogenesis; $Foxd3^{-/-}$ embryos fail around the time of implantation, cells of the inner cell mass cannot be maintained *in vitro*, and ES cell and trophoblast stem cell lines cannot be established (Hanna et al., 2002; Tompers et al., 2005). *In vivo*, the pool of both embryonic and trophoblast progenitors is not maintained without Foxd3; embryonic progenitor cells die while trophoblast progenitors give rise to an excess of trophoblast giant cells at the expense of the remaining trophoblast lineage. However, the ultimate effect in both cases is that the progenitor pool is not maintained and the cell lineage is lost.

Foxd3 is one of the earliest molecular markers of the NC lineage, it is expressed in multiple species in premigratory and migrating NC and expression is downregulated as the cells differentiate into most derivatives (Dottori et al., 2001; Labosky and Kaestner, 1998). Ectopic expression of Foxd3 in chick neural tube and Xenopus embryos can specify NC cell fate as measured by upregulation of HNK-1 and Slug (Dottori et al., 2001; Kos et al., 2001; Sasai et al., 2001). In addition, maintained expression of Foxd3 in migrating NC interferes with differentiation and retains NC in an undifferentiated state, evidence that points to a potential role for Foxd3 in the control of stem cell self-renewal (Dottori et al., 2001). Morpholino knockdown of zebrafish Foxd3 and mutations that affect Foxd3 expression in the zebrafish NC have deleterious effects on maintenance of the NC (Lister et al., 2006; Montero-Balaguer et al., 2006; Stewart et al., 2006).

Because the deletion of *Foxd3* results in embryonic lethality around the time of implantation, we employed Cre-loxP technology to delete the Foxd3 coding region specifically in NC. Here we demonstrate that without this transcriptional regulator the NC lineage fails to be maintained resulting in catastrophic loss of most NC derivatives. Mutant mice perish at birth with a cleft face, the PNS is severely reduced, and the ENS is not formed. Surprisingly, however, while the cardiac NC is greatly reduced early in embryogenesis, by midgestation most cardiac NC derivatives are normal with subtle defects in a small percentage of mutant embryos. We show that the mechanism of cellular loss of most of the NC is by a failure to maintain the progenitor pool as much of the premigratory and early migrating NC undergoes cell death. Cells that survive are able to migrate and differentiate normally but cannot completely compensate for the early loss of progenitors. Our data demonstrate that Foxd3 is required for maintenance of NC progenitor cells and taken together with our previous work, places Foxd3 in the unique role of maintaining the undifferentiated multipotent state of three completely divergent progenitor populations of the early mammalian embryo.

## Materials and Methods

### Construction of *Foxd3 floxP* Targeting Vector

A 1.2Kb fragment of the *Foxd3* locus was inserted into the *EcoR*1 site of pPNT4 downstream of the Frt-flanked *Neo* gene to serve as the 3′ homology arm. An oligonucleotide containing the loxP recognition sequence (ATAACTTCGTATAGCATACATTATACGAAGTTAT) was inserted 5′ of the *Foxd3* coding region. Upstream, a 4.2kb fragment of the *Foxd3* locus was inserted to complete the 5′ homology arm to generate the final targeting vector shown in Fig. 1A.

### ES Cell Electroporation and Generation of Mice

TL1 ES cells were electroporated as described (Tompers and Labosky, 2004). ES cell DNA was analyzed using Southern blot as shown in Fig. 1A and B. Lines were screened by PCR for the presence of the 5′ loxP site. We identified three correctly recombined cell lines out of 337 (0.9% frequency). Chimeras were generated by blastocyst injection and offspring of chimeras genotyped to identify heterozygous founders. Two independent cell lines transmitted through the germ line and because both showed the identical phenotype we restricted our studies to one cell line. Mice were genotyped either by Southern blot or PCR with the following primers: 5′ CGGCTTTCTTTCGGGGGAC3′ and 5′ACATATCGCTGGCGCTGCCG3′ to give a 130bp band for the wild type allele and a 220bp band for the floxed allele.

### Mouse Strains

*Foxd3*$^{tm2.Lby}$ is a null mutation of Foxd3 generated previously (Hanna et al., 2002) and is referred to as *Foxd3*$^{-}$ throughout. *Wnt1-Cre* mice were a generous gift of Drs. Andrew McMahon and David Rowitch. In the reporter strain *Gt(ROSA)26Sor*$^{tm1Sor}$ (referred to as *ROSA26R*) *Cre* expression results in removal of a *loxP*-flanked DNA segment that prevents expression of a *lacZ* gene. After *Cre* activation, *lacZ* is detected in cells/tissues where *Cre* is expressed. The transgenic line EIIaCre (Tg(EIIa-cre)C5379Lmgd from The Jackson Laboratories) carries a *Cre* transgene under control of the adenovirus EIIa promoter that targets expression of *Cre* recombinase to the early mouse embryo and acts as a ubiquitous deletor strain for our purposes. The presence of *Cre* was detected with primers: 5′ TGATGAGGTTCGCAAGAACC3′ and 5′CCATGAGTGAACGAACCTGG 3′ producing a band size of 400bp. All mouse strains were maintained on an outbred mixed genetic background that is primarily CD-1 and C57BL/6. Animals were maintained in accordance with the rules of the University of Pennsylvania and Vanderbilt University Institutional Animal Care and Use Committee (IACUC).

### Histology and whole mount in situ hybridization

Histology was performed using standard procedures (Presnell and Schreibman, 1997). For frozen sections (beta-galactosidase antibody only) embryos were fixed in 4% PFA in PBS overnight, equilibrated in 30% sucrose overnight and embedded in OCT. Sections were cut at 10 microns. For whole-mount LysoTracker staining, embryos were dissected in Hanks' buffer, and incubated in 5 hM LysoTracker (Molecular Probes) at 37°C for 1 hour. Embryos were then washed in Hanks' buffer and fixed in 4% PFA in PBS overnight, washed in PBS and dehydrated in methanol before imaging with a fluorescent stereoscope. TUNEL assay was performed in paraffin sections using the In Situ Cell Death Detection Kit (Roche). Whole-mount immunostaining was performed as described (Wall et al., 1992). Skeletal preparations and 5-bromo-4-chloro-3-indolyl -D-galactoside (Xgal) staining followed standard techniques (Nagy et al., 2003). For histological analysis, paraffin sections (7–12 microns) were counter-stained with eosin.

The following antibodies were used: rabbit-anti-Foxd3 at 1:1000 (Tompers et al., 2005); mouse-anti-PGP9.5 at 1:100 (Biogenesis), mouse-anti-neurofilament (2H3 monoclonal) at 1:1000 (Developmental Studies Hybridoma Bank), mouse-anti-beta III tubulin (Tuj1) at 1:100 (Chemicon), rabbit-anti-phosphohistone H3 at 1:200 (Upstate Biotechnology), goat-anti-FABP7 (also known as BFABP) at 1:20 (R&D), goat-anti-rabbit-Cy3, goat-anti-mouse-Cy3 and donkey-anti-goat-Cy2 (Jackson ImmunoResearch Laboratories). The Vectastain ABC kit (Vector Laboratories) was used to detect the non-fluorescent secondary antibodies and DAPI (1:5000 from Molecular Probes) was used to highlight nuclei.

Whole mount in situ hybridization was performed using Costar 12-well inserts following standard protocols (Hanna et al., 2002). Probes for *Crabp* (Stoner and Gudas, 1989), *Dlx1* (Dolle et al., 1992), *Msx1* (Satokata and Maas, 1994), *Pdgfa* (Mercola et al., 1990), *Pdgfc* (Ding et al., 2000), and *Sox10* (Southard-Smith et al., 1998) were as described. Digoxigenin labeled RNA probes were prepared using reagents from Roche Molecular Biochemicals.

Corrosion casting was performed as described (Feiner et al., 2001) by injecting the left ventricle of embryonic or newborn hearts first with PBS and then with polymer containing red pigment using gentle pressure (Polysciences #07349). Polymer containing blue pigment was injected into the right ventricle to monitor for possible ventricular septal defects (VSD). The casts cured overnight at 4 °C and surrounding tissue was macerated (Polysciences #07359) at 50 °C for 6–8 h.

## Results

### Conditional Deletion of the Foxd3 Locus in NC

A targeting vector was designed so that after homologous recombination in ES cells the *Foxd3* coding region (Fig. 1A purple box) would be flanked with loxP sequences (Fig. 1A orange triangles). Correctly targeted ES cells were used to generate mice carrying a $Foxd3^{flox}$ allele. Mice carrying two $Foxd3^{flox}$ alleles ($Foxd3^{flox/flox}$ mice) appeared normal and healthy. To test whether Cre-mediated deletion of the *Foxd3* locus produced a null allele efficiently, we crossed $Foxd3^{flox/flox}$ mice with $Foxd3^{flox/+}$; *EIIa-Cre* mice. Timed pregnant females from this cross were dissected at 6.5 days post coitum (dpc) and 25% of the resulting embryos had a phenotype identical to the original loss of function allele (data not shown). There was no difference in results observed with or without the *neo* selection cassette (data not shown).

To selectively delete *Foxd3* in the NC, we used the well-characterized *Wnt1-Cre* transgenic mouse line in which Cre recombinase is expressed in migrating NC starting at 8.0–8.5 dpc (Danielian et al., 1998). We used reciprocal matings between $Foxd3^{flox/flox}$ and $Foxd3^{+/-}$; *Wnt1-Cre* mice to obtain $Foxd3^{flox/-}$; *Wnt1-Cre* (mutant) embryos. At the four-somite stage (~8.0 dpc), Foxd3 protein is detected in migrating NC in the head folds (Fig. 1D). In contrast, we see a severe reduction in Foxd3 protein in head folds of mutant embryos, detecting only one or two cells that are weakly positive for Foxd3 protein expression (Fig. 1E, arrow). By 9.5 dpc, no Foxd3 protein is detected in the mutant dorsal neural tube or migratory path of NC (compare Fig. 1F and G). Foxd3 expression is not maintained in the facial mesenchyme at 13.5 dpc, expression is limited to forming cranial ganglia (Fig. 1H) and this expression is missing in mutant embryos. In the ENS, Foxd3 protein is expressed in the gut coils at 13.5 dpc and is missing in mutant embryos (Fig. 1J-K). These results demonstrate that *Foxd3* is deleted specifically in the NC by *Wnt1-Cre*.

## Maintenance of Cranial NC is Dependent on Foxd3

Initially, litters were allowed to progress to term and no mutant mice were found at weaning (21 days). However, we found one dead mutant newborn pup (pictured in Fig. 2A) and began monitoring litters before the mice were born (Table 1). While the majority of 18.5 dpc littermates appeared normal and could survive being delivered by a caesarian section, the mutant mice attempted to breathe several times but then expired. Table 1 summarizes the number of offspring and embryos from both *Foxd3*$^{flox/+}$ × *Foxd3*$^{+/-}$; *Wnt1-Cre* and *Foxd3*$^{flox/flox}$ × *Foxd3*$^{+/-}$; *Wnt1-Cre* crosses. Embryos were found in the expected ratios at all times in development and no mutant mice survived more than a few hours.

All mutant mice had a severe cleft face and palate incompatible with survival and their inability to breathe is presumably the cause of their death immediately after birth. These defects occurred with 100% penetrance although the width of the cleft sometimes varied in size. Nostrils and whisker pads were present but the facial midline never fused and the eyelids were partially open. Much of the skull vault is derived from cranial NC so we analyzed skeletons using Alcian Blue and Alizarin Red staining. Comparison of the control and mutant skulls in Fig. 2B revealed that the frontalnasal bone and nasal cartilage were missing in the mutants and the interparietal, parietal and basal occipital bones were greatly reduced in size. The maxilla and premaxila were shortened and the mandible was shortened and thickened. These cranial defects were obvious at midgestation stages (Fig. 2C).

To monitor NC and their derivatives, we introduced the *ROSA26R (R26R)* conditional reporter allele into the mutant background (Soriano, 1999). Upon expression of Cre protein, all cells and their descendants transcribe the *lacZ* gene, and therefore NC cell fate can be monitored directly with and without Foxd3 function. Note that we are comparing *Foxd3*$^{flox/-}$; *Wnt1-Cre; R26R* (mutant) embryos to *Foxd3*$^{flox/+}$; *Wnt1-Cre; R26R* (control) embryos so that the Cre protein will be recombining two sets of loxP sites; one to delete the *Foxd3* coding region and one to delete the stop sequence in the *ROSA26* locus. Xgal-positive tissue is present in the frontalnasal mesenchyme in both control and mutant embryos indicating that NC cells contribute to these tissues in the absence of Foxd3 (Fig 2D, Sup. Fig 3).

## Pharyngeal Arch Defects

At 9.5 dpc, a comparison of lineage-mapped embryos revealed that NC have migrated into pharyngeal arches (PA) 1 and 2 in both mutants and controls (Fig. 3A). However, by 10.5 dpc morphological differences in the PAs were apparent by SEM (Fig. 3B). The maxillary and the mandibular prominences of PA1 were present but reduced in size. There is a striking decrease of NC in PA 3 and 4. Immunohistochemistry for Neurofilament protein showed all cranial ganglia and nerves are present but smaller than normal. Some cranial nerves are slightly misdirected (the glossopharyngeal nerve in Fig. 3C) or have not extended as far as the control (the facial and vestibulocochlear nerves). Spinal nerves along the trunk of the mutant embryos were thinner. Examining expression of *Sox10*, a marker of early NC, revealed reduced expression in the developing trigeminal, facial and vestibulocochlear ganglia and no expression in the glossopharyngeal and vagus ganglia. *Sox10* expression was also reduced along the trunk of the embryo (Fig. 3D). Expression of other NC specific genes in the PAs uniformly showed reduced expression in PA 1 and 2 (Sup. Fig. 1). Together, these data suggest that the initial specification of NC occurs, but there is an overall failure to maintain NC progenitors as demonstrated by a loss of PA-derived structures and a concomitant decrease in expression of NC specific genes.

## Reduction of Peripheral Nervous System and Loss of Enteric Nervous System

NC migrate into the limbs during development giving rise to neurons, Schwann cells and terminal glia cells. Cutaneous nerves and the developing sciatic nerve are highlighted in a

hindlimb from a 14.5 dpc control embryo by Xgal lineage staining (Fig. 4A). All of these NC-derived cells are missing in the mutant embryos (Fig. 4B). A dorsal view of the same pair of embryos reveals the segmented pattern of spinal nerves exiting the dorsal root ganglia (DRG) and projecting ventrally in the control (Fig. 4C); the spinal nerves are absent in mutant embryos (Fig. 4D).

NC that migrate ventrally from the dorsal neural tube contribute to the ENS: the neurons and glia that innervate the entire gastrointestinal tract. Using the *ROSA26R* reporter allele, NC contribution to the ENS is easily visualized. In control midgestation embryos (14.5 dpc) the intestines are ensheathed in a plexus of NC-derived Xgal-positive cells while in a mutant littermate the gut is completely lacking these cells (Fig. 4E and F). When the gastrointestinal tract is dissected out of a 17.5dpc embryo, the control sample is surrounded in X-gal-positive cells along the entire anterior to posterior axis while the mutant sample has no NC-derived cells around the outside of the gut tube (Fig. 4G and H). Expression of PGP9.5 is readily detectable in neurons of the ENS in control embryos; there are no PGP9.5-positive cells in mutant embryos (Fig. 4I and J). Similar results were obtained with Tuj1 antiserum to detect neurons and FABP7 antiserum to detect glia (data not shown).

## Subtle Cardiac Neural Crest Defects

NC from the mid-otic placode to somite 4 migrate through rhombomeres 6–8, into PAs 3, 4 and 6, contributing to the aortic arch arteries and the aorticopulmonary septum of the cardiac outflow tract. In control embryos, NC enter PAs 3,4 and 6 (Fig 3A) and the developing heart field by 9.5 dpc (Fig. 5A arrows) and continue migrating at 10.5 dpc (Fig. 5B). We observed a striking decrease in the cardiac NC of mutant embryos. Fewer cells entered the heart field at 9.5 dpc (Fig. 5C). At 10.5 dpc, there is a paucity of NC in mutant PAs (Fig. 5D, arrow) and greatly reduced number of cells entering the heart (Fig. 5D, arrowhead).

To further investigate development of the cardiac NC we examined patterning of vascular NC derivatives using corrosion casting (Fig 5 E–H). We observed normal patterning of the aortic arch in the majority of *Foxd3* mutants (13/17, 76%) between 15.5 dpc until birth. However, in 3 out of 17 *Foxd3* mutant embryos examined, we observed a duplication of the left common carotid artery (Fig 5 G and G′). One mutant embryo had severe cardiac NC defects including type A2 persistent truncus arteriosis (PTA) in which the septation of the outflow tract did not occur and the ductus arteriosis was absent (Fig 5H-H′) (Van Praagh and Van Praagh, 1965). We examined the NC lineage in both control and mutant embryos with the *ROSA26R* reporter allele and saw no differences in NC contribution to the cardiovascular system at 17.5 dpc (n = 7 mutants, Sup. Fig. 2). Histological analysis of eight mutant and control littermates was performed and no septal defects were observed (Sup. Fig. 2), however, while in the process of performing resin casts, 1/17 (the sample shown in Fig. 5H) displayed a ventricular septal defect.

## NC Cell Migration, Differentiation, Death, and Proliferation

NC must maintain a delicate balance of proliferation and migration, and timing of differentiation is crucial for their final tissue contributions in the adult. Lineage tracing revealed that DRGs were formed (Fig. 6A and B) but were smaller than normal. The size of the DRGs varies with the angle of section, but in whole mount, mutant DRGs are consistently smaller than controls (Fig. 3A). However, a more ventral field of the same region revealed that while control NC enter the foregut to eventually populate the ENS (Fig. 6C), mutant NC are fewer in number and halt their migration near the dorsal aorta in a position consistent with the final location of sympathetic ganglia (Fig. 6D). No mutant NC enter the developing gut anywhere along the anterior-posterior axis.

Terminal differentiation of NC occurs as cells reach their final destination. We detected expression of neural and glial markers in control and mutant DRGs. At 9.5 and 14.5 dpc, the neural marker beta III tubulin and the glial marker FABP7 (also called B-FABP) are expressed in both control and mutant DRGs (Fig. 6E–H and data not shown).

We examined cell death in control and mutant embryos and detected an increase in TUNEL-positive apoptotic cells in the dorsal spinal cord while there were few, if any, TUNEL-positive cells in the spinal cord of control embryos (Fig. 6I and J). Confirming this with LysoTracker® Red dye, at 9.0 dpc, mutant embryos showed increased apoptosis in the hindbrain and by 10.5 dpc, apoptosis was more pronounced in the posterior tail of the embryo (Figure 6 K-N). The absence of apoptosis in distal PAs of mutant embryo at 10.5 dpc (Fig 6M) is likely due to the large deficit in NC cell numbers (note morphology of PAs in Fig. 6M and lineage label in Fig. 3B).

To more closely examine the curious recovery of most of the cardiac derivates we analyzed cell proliferation in the cardiac NC using a combination of lineage labeling and immunohistochemistry for phosphorylated histone H3 protein indicating cells in mitosis. Septation is complete by 13.0 dpc so we chose to examine embryos at 12.5 dpc (Hiruma et al., 2002). Representative sections of 12.5 dpc control and mutant embryos are shown in Fig. 6 O-R clearly demonstrating the paucity of NC present in the outflow tract at most rostral and caudal levels. The volume of the outflow tract control and mutant embryos was calculated as 4 $mm^3$ and 0.7 $mm^3$, respectively. The proportion of pH3-positive NC cells was not different between controls and mutants (details in Sup. Fig. 3). These results suggest that although loss of Foxd3 reduced the number of cardiac NC, these cells are still able to pattern the outflow tract and give rise to smooth muscle cells.

## Discussion

### NC Specification

Previous data from several laboratories has demonstrated that ectopic expression of Foxd3 in the neural tube can change the fate of the neuroepithelium into NC (Cheung et al., 2005; Dottori et al., 2001; Kos et al., 2001; Sasai et al., 2001). However, our loss-of-function analysis suggests that Foxd3 is not required for the initial specification of the NC. In *Foxd3$^{flox/-}$; Wnt1-Cre* mutant embryos, we do not detect cells expressing Foxd3 at the earliest stages of NC specification (Fig. 1D–G) yet there are still NC present (Fig. 3). There remains the possibility that the *Wnt1-Cre* transgene does not produce Cre protein early enough and there may be a few Foxd3 expressing cells present, but if so, our data show that they are not maintained. It is more likely that the role of Foxd3 is in maintaining the NC, not in specifying this cell type.

Our findings do not completely agree with those of other model systems, highlighting differences between *Xenopus*, chick, zebrafish and mouse NC. Ectopic expression of a dominant negative FoxD3 in *Xenopus* embryos suppresses NC specification as measured by the loss of NC marker expression (Sasai et al., 2001). Electroporation of antisense oligonucleotides specific to Foxd3 in the chick bias the differentiation of NC towards the melanocyte lineage (Kos et al., 2001). There are three recent reports of mutations in the zebrafish *Foxd3* locus or knockdown of Foxd3 using morpholinos (Lister et al., 2006; Montero-Balaguer et al., 2006; Stewart et al., 2006). These groups reported that NC was specified normally with a general downregulation of NC markers similar to what we have observed. Craniofacial defects were highlighted by jaw abnormalities in the fish while defects in the mandible of our mice were minor. All three groups demonstrated a complete loss of DRGs while we see smaller DRGs that contain neurons and glia. Similar to what we observe, in all cases the zebrafish ENS was lost and increased cell death in the NC lineage was observed along with defects in migration. Zebrafish are an ideal system to monitor changes in different types

of NC melanocytes and all three groups described lineage specific differences in these derivatives. For example, in the *Mother Superior* mutation, which is a mutation somewhere outside the coding region that affects only NC expression of Foxd3, melanophores are delayed in their development but then recover while iridophores remain greatly reduced (Montero-Balaguer et al., 2006). Zebrafish cardiac NC contributes primarily to the myocardial cell lineage (Li et al., 2003). Despite this, only one group reported a slight edema in the heart in *Foxd3* mutants (Montero-Balaguer et al., 2006).

## NC Patterning

We did not detect anterior-posterior patterning defects in NC although caudal NC was most severely affected. All mutant embryos had severe facial clefting and were missing many NC-derived facial bones. However, the mandible was present in all mutants examined. It was shortened and thickened similar to *Dlx5*$^{-/-}$ mice (Acampora et al., 1999), but its presence demonstrates that *Foxd3*$^{-/-}$ NC can differentiate into cartilage and bone and overt cranial patterning is unaltered. Similarly, trunk NC were present in reduced numbers, but those cells migrated away from the neural tube normally and formed small DRGs that contained both neurons and glia.

In contrast, the vagal and sacral NC destined to contribute to the ENS did not migrate to the gut. There are several possibilities for the loss of this sub-lineage of NC. One hypothesis is that there may be expression of closely related *Fox* genes in the cranial and cardiac NC but no such compensating family members expressed in the trunk NC caudal to somite 7. A second hypothesis is that ENS progenitors underwent selective cell death in the dorsal neural tube while NC destined to populate the DRGs were maintained. There are no molecular markers to distinguish these lineages prior to migration so we cannot test this hypothesis directly. A third possibility is that NC that underwent apoptosis in the dorsal neural tube were unspecified and the selective loss of the ENS-NC is because this lineage must migrate farther than others. Therefore a general loss in progenitor cell number might affect the ENS-crest more severely. A fourth possibility is that *Foxd3*$^{-/-}$ NC might not be able to enter the foregut (Fig. 6C compared to D). It has been demonstrated that vagal and sacral NC, unlike the rest of the trunk NC, possess a unique ability to enter the gut mesentery (Serbedzija et al., 1991). Recent studies suggest this difference might be at least partially explained by the expression of axon guidance molecules Slit and Robo on vagal NC (De Bellard et al., 2003). In contrast to our results, mice lacking members of the glial cell line-derived neurotrophic factor signaling pathway have enteric neurons in the anterior ENS (Cacalano et al., 1998;Pichel et al., 1996;Sanchez et al., 1996) while mutations in Endothelin-3 or Endothelin Receptor B cause the loss of ENS only in the distal colon (Baynash et al., 1994;Hosoda et al., 1994). In *Phox2b*$^{-/-}$ embryos, there is an initial migration of vagal NC into the proximal gut mesentery, but these progenitors are not maintained leaving the entire gut without innervation (Pattyn et al., 1999). In fact, the only other mouse model lacking the entire ENS is *Sox10*$^{Dom/Dom}$ (Kapur, 1999;Southard-Smith et al., 1998) and it is interesting to note that Sox10 is one of the genes severely downregulated in *Foxd3*$^{-/-}$ mutant embryos (Fig. 3C arrowheads). One final hypothesis, not mutually exclusive of those suggested above, is that while Foxd3 appears to be equally expressed throughout the early premigratory crest, it might be differentially required in specific subpopulations of the crest.

Our surprising results showing the minimal phenotype of the mutant cardiac NC supports this last hypothesis. The cardiac crest normally migrates into PA 3, 4 and 6, eventually contributing to the cardiac outflow tract and the aorticopulmonary septum. There is a striking reduction of cardiac NC in PA 3, 4 and 6 in mutant embryos compared to controls (Figs 3A and 5 A–D). However, this greatly reduced population of cardiac NC migrates into the heart field and even though there are far fewer cells (mutants contained 18% the volume of NC compared to controls

by lineage label), this reduced number can effectively septate the outflow tract in most cases. We did not observe alterations from the wild type pattern of proliferation as monitored by phosphorylated histone 3 protein at 9.5 dpc. This suggests that the extent of migration of the cardiac NC, rather than the number of cardiac NC cells, is crucial for their ability to effectively septate the outflow tract. One of our future goals is to understand molecular differences between the cardiac NC, which can overcome the loss of Foxd3, and the rest of the NC lineage that is dependent on this transcription factor.

### Conservation of Foxd3 function in progenitor cells

Development of all embryonic tissues relies on progenitor cells that are able to self-renew and differentiate appropriately. Our initial description of the *Foxd3*$^{-/-}$ phenotype demonstrated that this protein is required for maintenance of epiblast cells and therefore required for establishing ES cells (Hanna et al., 2002). Foxd3 is similarly required in the trophoblast progenitor lineage (Tompers et al., 2005), a lineage completely disparate from the embryonic one primarily affected in the null mutation. Therefore, the NC is the third multipotent lineage that requires Foxd3 for maintenance of progenitor cells, making an unprecedented molecular connection between these three distinct progenitor populations. These lineages are embryonically-derived and we have yet to demonstrate that Foxd3 can play a similar role in adult-derived stem cells. However, our results support the premise that certain self-renewal mechanisms are likely to be conserved in very different progenitor lineages. There are several other proteins known to regulate multiple progenitor lineages. Bmi1 and other polycomb proteins repress genes that induce cell death in the hematopoetic lineages, neural stem cells, NC stem cells and cancer stem cells (reviewed in (Pardal et al., 2005). Most recently, the transcription factor Zfx is required for self-renewal of ES cells and maintenance of adult hematopoietic stem cells (Galan-Caridad et al., 2007). The proto-oncogene *c-Myc* has a well documented role in cell proliferation; recent work in *Xenopus* suggests it may be involved in NC formation while genetic studies in the mouse show that a NC deletion of *Myc* results in a relatively mild phenotype (Bellmeyer et al., 2003; Wei et al., 2007). In addition to its role in NC development, expression of Myc along with several other “stem cell proteins” is sufficient to change the fate of somatic cells into pluripotent stem cells (Takahashi and Yamanaka, 2006). Finally, Sox2 is required in ES cells, TS cells and embryonic neural lineages (Avilion et al., 2003; Graham et al., 2003). Sox2 is also expressed in early migrating NC, in Schwann cells (Larysa Pevny, personal communication) and in the postnatal ENS (Vohra et al., 2006), all regions competent to give rise to NC stem cells. The role of Sox2 in the NC has not been investigated, and it is tempting to speculate that there may be a genetic interaction between Foxd3 and Sox2.

It is not clear how Foxd3 functions to maintain these progenitor pools. The protein can function as either an activator or a repressor in different contexts; in Xenopus mesoderm induction, Foxd3 recruits Groucho4 to repress target genes (Steiner et al., 2006; Yaklichkin et al., 2007) while in zebrafish somite maturation, Foxd3 activates Myf5 expression directly (Lee et al., 2006). We can not rule out that Foxd3 may behave similarly to Foxa proteins in modifying chromatin structure to allow access for other co-repressors or activators to target genes (Cirillo et al., 2002). Our major challenges ahead are to identify Foxd3 target genes and to determine the signaling pathways in which the protein functions.

## Supplementary Material

Refer to Web version on PubMed Central for supplementary material.

## Acknowledgements

The authors would like to thank Jonathan Epstein, Chris Brown and Diego Porras for analysis of the cardiac defect, Larysa Pevny for communicating unpublished data, Andrew McMahon and David Rowitch for providing *Wnt1-Cre* mice, Bruce Appel for use of his fluorescent stereomicroscope for imaging Lysotracker staining, Monika Kumanova for blastocyst injection and Alison LeGrone, Rachel Klein, Shang-Jui Wang and Jessica Yuan for technical help. Thanks to Marianne Bronner-Fraser, Brigid Hogan, Rulang Jiang, Randy Johnson, Moisés Mallo and Philippe Soriano for in situ probes. Thanks also to Leigh Compton, Brian Nelms, Jean-Pierre Saint-Jeannet, Vivian Siegel, Michelle Southard-Smith and Chris Wright for their thoughtful comments on the manuscript. This work was supported by grants from the American Heart Association and the NIH (HD36720) to PAL and an AHA predoctoral fellowship to NAM.

## References

Acampora D, Merlo GR, Paleari L, Zerega B, Postiglione MP, Mantero S, Bober E, Barbieri O, Simeone A, Levi G. Craniofacial, vestibular and bone defects in mice lacking the Distal-less-related gene Dlx5. Development 1999;126:3795–809. [PubMed: 10433909]

Avilion AA, Nicolis SK, Pevny LH, Perez L, Vivian N, Lovell-Badge R. Multipotent cell lineages in early mouse development depend on SOX2 function. Genes Dev 2003;17:126–40. [PubMed: 12514105]

Baynash AG, Hosoda K, Giaid A, Richardson JA, Emoto N, Hammer RE, Yanagisawa M. Interaction of endothelin-3 with endothelin-B receptor is essential for development of epidermal melanocytes and enteric neurons. Cell 1994;79:1277–85. [PubMed: 8001160]

Bellmeyer A, Krase J, Lindgren J, LaBonne C. The protooncogene c-myc is an essential regulator of neural crest formation in xenopus. Dev Cell 2003;4:827–39. [PubMed: 12791268]

Cacalano G, Farinas I, Wang LC, Hagler K, Forgie A, Moore M, Armanini M, Phillips H, Ryan AM, Reichardt LF, et al. GFRalpha1 is an essential receptor component for GDNF in the developing nervous system and kidney. Neuron 1998;21:53–62. [PubMed: 9697851]

Cheung M, Briscoe J. Neural crest development is regulated by the transcription factor Sox9. Development. 2003

Cheung M, Chaboissier MC, Mynett A, Hirst E, Schedl A, Briscoe J. The transcriptional control of trunk neural crest induction, survival, and delamination. Dev Cell 2005;8:179–92. [PubMed: 15691760]

Cirillo LA, Lin FR, Cuesta I, Friedman D, Jarnik M, Zaret KS. Opening of compacted chromatin by early developmental transcription factors HNF3 (FoxA) and GATA-4. Mol Cell 2002;9:279–89. [PubMed: 11864602]

Danielian PS, Muccino D, Rowitch DH, Michael SK, McMahon AP. Modification of gene activity in mouse embryos in utero by a tamoxifen-inducible form of Cre recombinase. Curr Biol 1998;8:1323–6. [PubMed: 9843687]

De Bellard ME, Rao Y, Bronner-Fraser M. Dual function of Slit2 in repulsion and enhanced migration of trunk, but not vagal, neural crest cells. J Cell Biol 2003;162:269–79. [PubMed: 12876276]

Ding H, Wu X, Kim I, Tam PP, Koh GY, Nagy A. The mouse Pdgfc gene: dynamic expression in embryonic tissues during organogenesis. Mech Dev 2000;96:209–13. [PubMed: 10960785]

Dolle P, Price M, Duboule D. Expression of the murine Dlx-1 homeobox gene during facial, ocular and limb development. Differentiation 1992;49:93–9. [PubMed: 1350766]

Dottori M, Gross MK, Labosky P, Goulding M. The winged-helix transcription factor Foxd3 suppresses interneuron differentiation and promotes neural crest cell fate. Development 2001;128:4127–38. [PubMed: 11684651]

Epstein DJ, Vekemans M, Gros P. Splotch (Sp2H), a mutation affecting development of the mouse neural tube, shows a deletion within the paired homeodomain of Pax-3. Cell 1991;67:767–74. [PubMed: 1682057]

Feiner L, Webber AL, Brown CB, Lu MM, Jia L, Feinstein P, Mombaerts P, Epstein JA, Raper JA. Targeted disruption of semaphorin 3C leads to persistent truncus arteriosus and aortic arch interruption. Development 2001;128:3061–70. [PubMed: 11688556]

Galan-Caridad JM, Harel S, Arenzana TL, Hou ZE, Doetsch FK, Mirny LA, Reizis B. Zfx controls the self-renewal of embryonic and hematopoietic stem cells. Cell 2007;129:345–57. [PubMed: 17448993]

Graham V, Khudyakov J, Ellis P, Pevny L. SOX2 functions to maintain neural progenitor identity. Neuron 2003;39:749–65. [PubMed: 12948443]

Hanna LA, Foreman RK, Tarasenko IA, Kessler DS, Labosky PA. Requirement for Foxd3 in maintaining pluripotent cells of the early mouse embryo. Genes Dev 2002;16:2650–61. [PubMed: 12381664]

Hiruma T, Nakajima Y, Nakamura H. Development of pharyngeal arch arteries in early mouse embryo. J Anat 2002;201:15–29. [PubMed: 12171473]

Hosoda K, Hammer RE, Richardson JA, Baynash AG, Cheung JC, Giaid A, Yanagisawa M. Targeted and natural (piebald-lethal) mutations of endothelin-B receptor gene produce megacolon associated with spotted coat color in mice. Cell 1994;79:1267–76. [PubMed: 8001159]

Kapur RP. Early death of neural crest cells is responsible for total enteric aganglionosis in Sox10(Dom)/Sox10(Dom) mouse embryos. Pediatr Dev Pathol 1999;2:559–69. [PubMed: 10508880]

Kos R, Reedy MV, Johnson RL, Erickson CA. The winged-helix transcription factor FoxD3 is important for establishing the neural crest lineage and repressing melanogenesis in avian embryos. Development 2001;128:1467–79. [PubMed: 11262245]

Labosky PA, Kaestner KH. The winged helix transcription factor Hfh2 is expressed in neural crest and spinal cord during mouse development. Mech Dev 1998;76:185–90. [PubMed: 9767163]

Labosky PA, Kaestner KH. Winged Helix transcription factors. Encyclopedic Reference of Genomics and Proteomics in Molecular Medicine. 2005

Le Douarin, NM.; Kalcheim, C. The Neural Crest. Cambridge: Cambridge University Press; 1999.

Lee HC, Huang HY, Lin CY, Chen YH, Tsai HJ. Foxd3 mediates zebrafish myf5 expression during early somitogenesis. Dev Biol 2006;290:359–72. [PubMed: 16386728]

Li YX, Zdanowicz M, Young L, Kumiski D, Leatherbury L, Kirby ML. Cardiac neural crest in zebrafish embryos contributes to myocardial cell lineage and early heart function. Dev Dyn 2003;226:540–50. [PubMed: 12619138]

Lister JA, Cooper C, Nguyen K, Modrell M, Grant K, Raible DW. Zebrafish Foxd3 is required for development of a subset of neural crest derivatives. Dev Biol 2006;290:92–104. [PubMed: 16364284]

Mercola M, Wang CY, Kelly J, Brownlee C, Jackson-Grusby L, Stiles C, Bowen-Pope D. Selective expression of PDGF A and its receptor during early mouse embryogenesis. Dev Biol 1990;138:114–22. [PubMed: 2155144]

Montero-Balaguer M, Lang MR, Sachdev SW, Knappmeyer C, Stewart RA, De La Guardia A, Hatzopoulos AK, Knapik EW. The mother superior mutation ablates foxd3 activity in neural crest progenitor cells and depletes neural crest derivatives in zebrafish. Dev Dyn 2006;235:3199–212. [PubMed: 17013879]

Nagy, A.; Gertsenstein, M.; Ventersten, K.; Behringer, R. Manipulating the Mouse Embryo: A Laboratory Manual. Cold Spring Harbor, NY: Cold Spring Harbor Laboratory Press; 2003.

Pardal R, Molofsky AV, He S, Morrison SJ. Stem cell self-renewal and cancer cell proliferation are regulated by common networks that balance the activation of proto-oncogenes and tumor suppressors. Cold Spring Harb Symp Quant Biol 2005;70:177–85. [PubMed: 16869752]

Pattyn A, Morin X, Cremer H, Goridis C, Brunet JF. The homeobox gene Phox2b is essential for the development of autonomic neural crest derivatives. Nature 1999;399:366–70. [PubMed: 10360575]

Pichel JG, Shen L, Sheng HZ, Granholm AC, Drago J, Grinberg A, Lee EJ, Huang SP, Saarma M, Hoffer BJ, et al. Defects in enteric innervation and kidney development in mice lacking GDNF. Nature 1996;382:73–6. [PubMed: 8657307]

Presnell, JK.; Schreibman, MP. Humason's Animal Tissue Techniques. Baltimore, MD: The Johns Hopkins University Press; 1997.

Sanchez MP, Silos-Santiago I, Frisen J, He B, Lira SA, Barbacid M. Renal agenesis and the absence of enteric neurons in mice lacking GDNF. Nature 1996;382:70–3. [PubMed: 8657306]

Sasai N, Mizuseki K, Sasai Y. Requirement of FoxD3-class signaling for neural crest determination in Xenopus. Development 2001;128:2525–36. [PubMed: 11493569]

Satokata I, Maas R. Msx1 deficient mice exhibit cleft palate and abnormalities of craniofacial and tooth development. Nat Genet 1994;6:348–56. [PubMed: 7914451]

Schorle H, Meier P, Buchert M, Jaenisch R, Mitchell PJ. Transcription factor AP-2 essential for cranial closure and craniofacial development. Nature 1996;381:235–8. [PubMed: 8622765]

Serbedzija GN, Burgan S, Fraser SE, Bronner-Fraser M. Vital dye labelling demonstrates a sacral neural crest contribution to the enteric nervous system of chick and mouse embryos. Development 1991;111:857–66. [PubMed: 1879357]

Soriano P. Generalized lacZ expression with the ROSA26 Cre reporter strain. Nat Genet 1999;21:70–1. [PubMed: 9916792]

Southard-Smith EM, Kos L, Pavan WJ. Sox10 mutation disrupts neural crest development in Dom Hirschsprung mouse model. Nat Genet 1998;18:60–4. [PubMed: 9425902]

Steiner AB, Engleka MJ, Lu Q, Piwarzyk EC, Yaklichkin S, Lefebvre JL, Walters JW, Pineda-Salgado L, Labosky PA, Kessler DS. FoxD3 regulation of Nodal in the Spemann organizer is essential for Xenopus dorsal mesoderm development. Development 2006;133:4827–38. [PubMed: 17092955]

Steventon B, Carmona-Fontaine C, Mayor R. Genetic network during neural crest induction: from cell specification to cell survival. Semin Cell Dev Biol 2005;16:647–54. [PubMed: 16084743]

Stewart RA, Arduini BL, Berghmans S, George RE, Kanki JP, Henion PD, Look AT. Zebrafish foxd3 is selectively required for neural crest specification, migration and survival. Dev Biol 2006;292:174–88. [PubMed: 16499899]

Stoner CM, Gudas LJ. Mouse cellular retinoic acid binding protein: cloning, complementary DNA sequence, and messenger RNA expression during the retinoic acid-induced differentiation of F9 wild type and RA-3-10 mutant teratocarcinoma cells. Cancer Res 1989;49:1497–504. [PubMed: 2538228]

Sutton J, Costa R, Klug M, Field L, Xu D, Largaespada DA, Fletcher CF, Jenkins NA, Copeland NG, Klemsz M, et al. Genesis, a winged helix transcriptional repressor with expression restricted to embryonic stem cells. J Biol Chem 1996;271:23126–33. [PubMed: 8798505]

Takahashi K, Yamanaka S. Induction of pluripotent stem cells from mouse embryonic and adult fibroblast cultures by defined factors. Cell 2006;126:663–76. [PubMed: 16904174]

Tompers DM, Foreman RK, Wang Q, Kumanova M, Labosky PA. Foxd3 is required in the trophoblast progenitor cell lineage of the mouse embryo. Dev Biol 2005;285:126–37. [PubMed: 16039639]

Tompers DM, Labosky PA. Electroporation of murine embryonic stem cells: a step-by-step guide. Stem Cells 2004;22:243–9. [PubMed: 15153600]

Van Praagh R, Van Praagh S. The anatomy of common aorticopulmonary trunk (truncus arteriosus communis) and its embryologic implications. A study of 57 necropsy cases. Am J Cardiol 1965;16:406–25. [PubMed: 5828135]

Vohra BP, Tsuji K, Nagashimada M, Uesaka T, Wind D, Fu M, Armon J, Enomoto H, Heuckeroth RO. Differential gene expression and functional analysis implicate novel mechanisms in enteric nervous system precursor migration and neuritogenesis. Dev Biol 2006;298:259–71. [PubMed: 16904662]

Wall NA, Jones CM, Hogan BL, Wright CV. Expression and modification of Hox 2.1 protein in mouse embryos. Mech Dev 1992;37:111–20. [PubMed: 1353982]

Wei K, Chen J, Akrami K, Galbraith GC, Lopez IA, Chen F. Neural crest cell deficiency of c-myc causes skull and hearing defects. Genesis 2007;45:382–90. [PubMed: 17523175]

Wijchers PJ, Burbach JP, Smidt MP. In control of biology: of mice, men and Foxes. Biochem J 2006;397:233–46. [PubMed: 16792526]

Yaklichkin S, Steiner AB, Lu Q, Kessler DS. FoxD3 and Grg4 physically interact to repress transcription and induce mesoderm in Xenopus. J Biol Chem 2007;282:2548–57. [PubMed: 17138566]

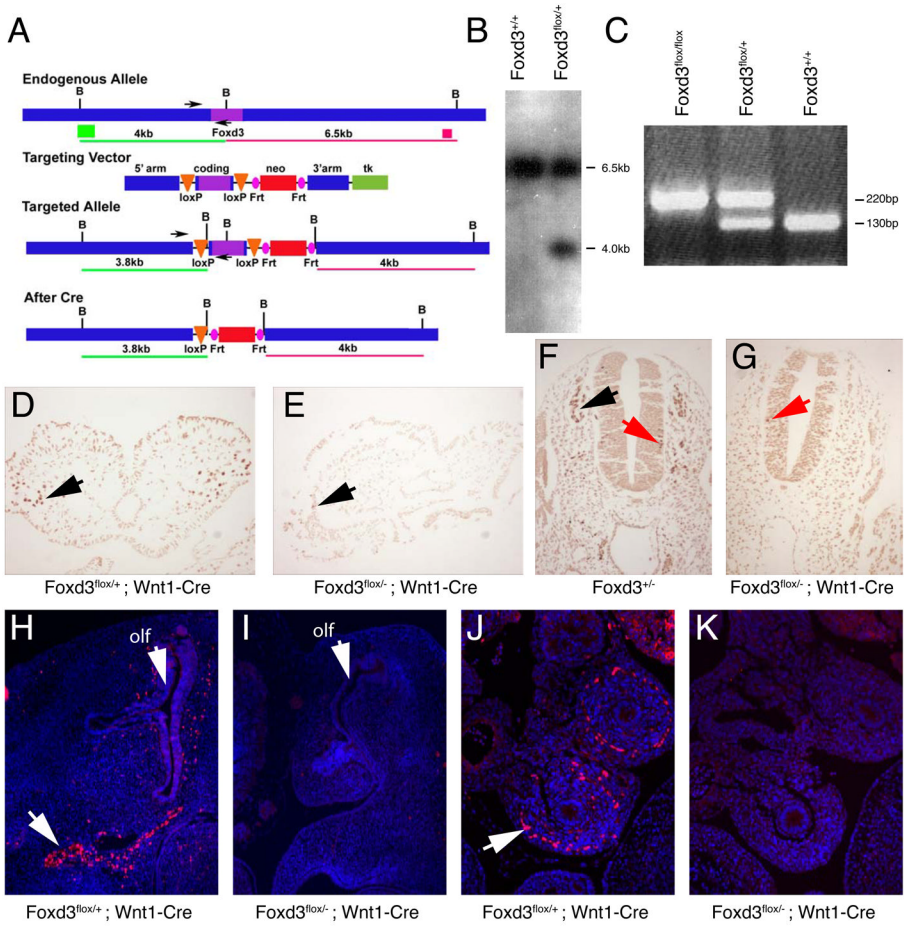


**Figure 1. Generation of a NC specific deletion in *Foxd3***

**A.** *Foxd3* locus, targeting vector and resulting alleles. Purple box indicates the single coding exon. **B.** Southern blot analysis using 3′ probe shown in A with *BamH*1 digested genomic DNA. 6.5kb wild type band and correctly targeted 4kb band are indicated. **C.** Genotyping mice with PCR primers (black arrows in A). PCR product from *Foxd3* floxed allele is 220 bp, wild type allele 130 bp. **D–K.** Foxd3 Immunohistochemistry. In a control embryo, NC express Foxd3 at 8 dpc in the headfolds (D), at 9.5 dpc in migrating NC (F) (black arrow), at 13.5 in cranial nerves (H) (white arrow) and in the gut coils (J) (white arrow). In E, Foxd3 protein is detected in a few cells in headfolds of a mutant 8 dpc embryo (black arrow). In contrast, no Foxd3 expression is detected at 9.5 dpc in the trunk of a mutant embryo (G) or in the cranial nerves (I) or gut coils (K) at 13.5 dpc. Foxd3 expressing ventral interneurons are detected in the neural tube of control and mutant embryos (red arrows in F and G).
bp, base pairs; olf, olfactory epithelium.

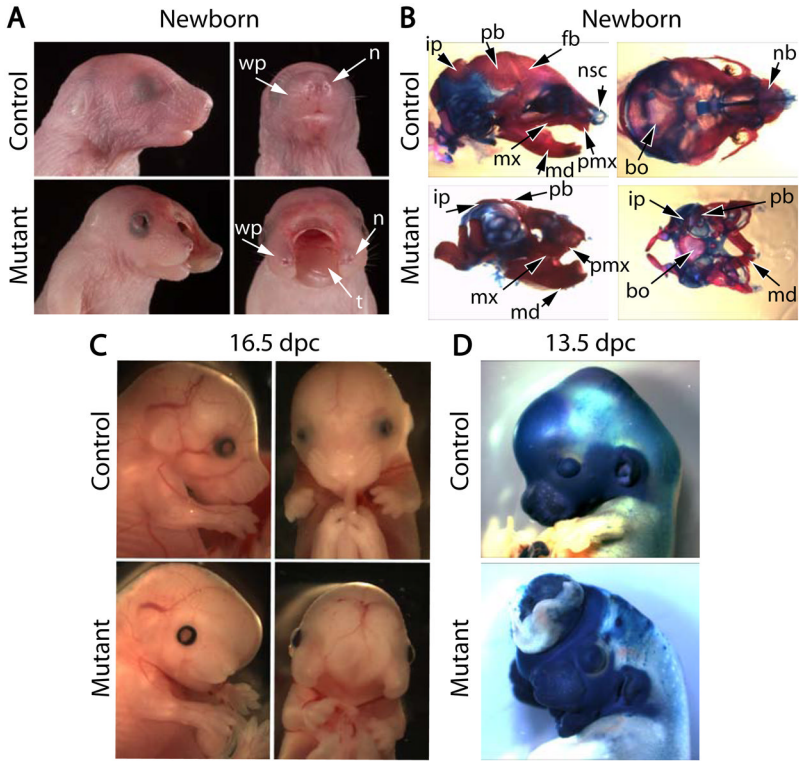


**Figure 2. Craniofacial dysmorphogenesis, skeletal abnormalities and PA malformations in *Foxd3*$^{flox/-}$; *Wnt1-Cre* mice and embryos**

**A**. Newborn mutant mice were found with a severe cleft face and palate. **B**. Alizarin Red and Alcian Blue staining of the head skeleton and cartilage, lateral and dorsal views. The frontal bone and nasal capsule are missing in mutants and the parietal and interparietal bones are greatly reduced in size. The basioccipital bone and premaxila are present but smaller and the mandible is shortened and thickened. **C**. Side and front view of embryos at 16.5 dpc shows these defects at midgestation. **D**. Side view of lineage labeled (*R26R*) embryos showing the contribution of NC to the face at 13.5 dpc in control and mutant embryos.

bo, basioccipital bone; fb, frontal bone; ip, interparietal bone; md, mandible; mx, maxilla; n, nostrils; nb, nasal bone; nsc, nasal capsule; PA1md, mandibular prominence of pharyngeal arch 1; PA1mx, maxillary prominence of pharyngeal arch 1; PA2, pharyngeal arch 2; pb, parietal bone; pmx, premaxilla; t, tongue; wp, whisker pads.

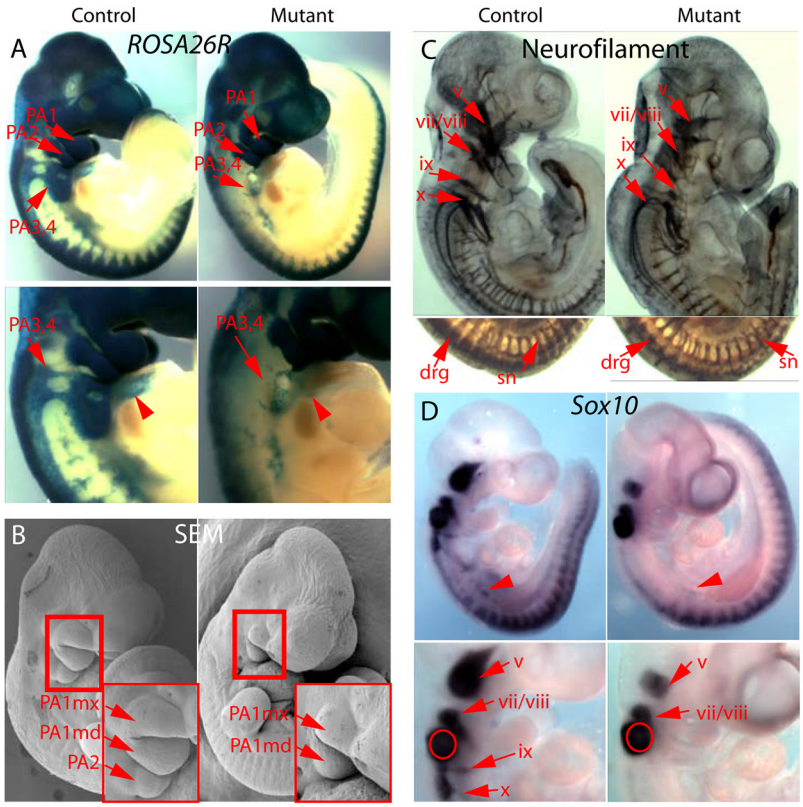


**Figure 3. Pharyngeal Arch Defects in *Foxd3*$^{flox/-}$; *Wnt1-Cre* embryos**

**A.** Beta-galactosidase activity as detected by Xgal staining in control and mutant embryos at 9.5 dpc. PA 1 and 2 are present but smaller in mutants and there is a paucity of cells migrating into PA 3–4 and into the developing cardiac region (arrowheads). **B.** Scanning electron micrographs of 10.5 dpc embryos showing PA deficiency. Embryos were matched for somite number. **C.** Whole mount antibody staining of Neurofilament protein. Cranial nerves are present in mutants but smaller and slightly misdirected. In the trunk (lower panels), the mutant embryo has smaller DRG and thinner spinal nerves than the control. Note, these embryos have been cleared so both left and right nerves are visible. **D**. Whole mount in situ hybridization of embryos for *Sox10.* In mutant embryos, *Sox10* mRNA is not detected in the glossopharyngeal (IX) and vagus (X) ganglia although it is detected at reduced levels in the trigeminal (V), facial (VII) and vestibulocochlear (VIII) ganglia. Signal is also missing in the foregut of mutants (arrowheads). Signal in the otic vesicle (circled) is background.

drg, dorsal root ganglion; v, trigeminal ganglion; vii, facial ganglion; viii vestibulocochlear ganglion; ix, glossopharyngeal ganglion; x, vagus ganglion; PA, pharyngeal arch; sn, spinal nerves.

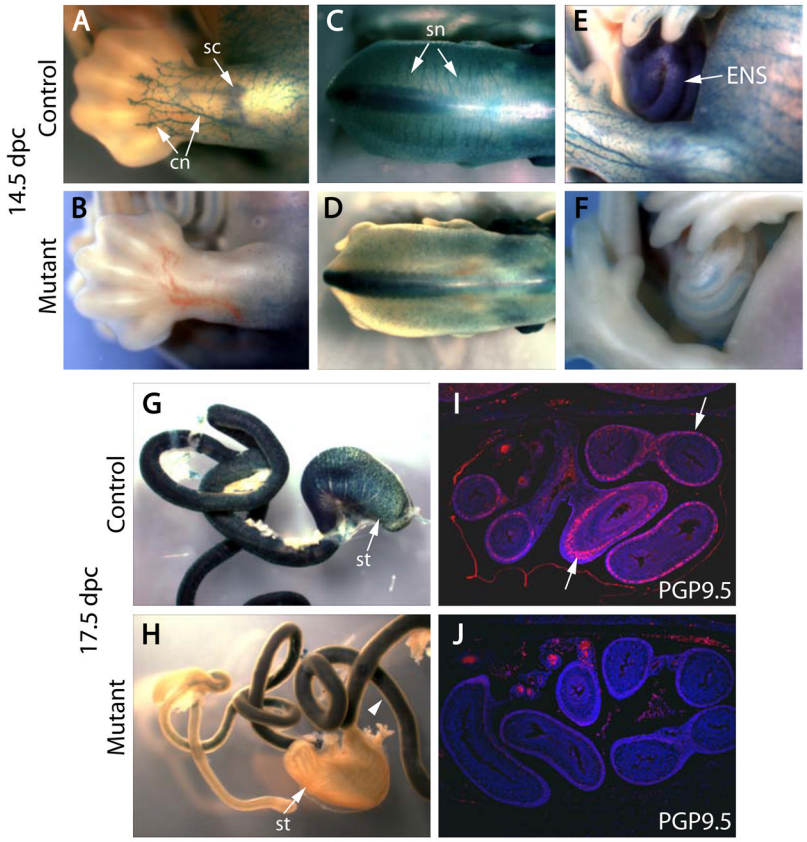


**Figure 4. Peripheral and Enteric Nervous System Defects in *Foxd3*$^{flox/-}$; *Wnt1-Cre* embryos**

**A-H.** Beta-galactosidase activity detected by Xgal staining in control and mutant embryos. **A**–**B.** Lateral view of hindlimbs of 14.5 dpc embryos. In control embryos, development of cutaneous nerves is obvious and the developing sciatic nerve is visible (A). None of these structures are seen in mutant embryos (B). **C**–**D.** Dorsal view of the trunk a control embryo at 14.5 dpc shows the segmented development of spinal nerves radiating out from the developing spinal cord (C). This is not seen in mutant embryos (D). **E**–**F.** Lateral view of a 14.5 dpc embryo shows coils of the developing gastrointestinal tract. In the control embryo, cells of the ENS stain blue on the outside of the gut coils (E). In the mutant embryo no blue staining of the ENS is visible and the absence of cutaneous peripheral nerves is apparent (F). **G**–**H.** Dissected gastrointestinal tracts from 17.5 dpc embryos. In the control, the entire extent of the gut is ensheathed in NC-derived cells making up the ENS (G). In the mutant, there are no X-gal-positive cells around the outside of the gut (H). Blue staining inside the lumen is background (arrowhead). **I**–**J.** Immunofluorescence for PGP9.5, a protein enriched in neurons, shows location of the ENS neurons in cross sections of the intestine in the control embryo (I) while no PGP9.5 signal is detected in the mutant (J). PGP9.5 signal is red, sections were counterstained with DAPI in blue to reveal nuclei.

cn, cutaneous nerves; ENS, enteric nervous system; sc, sciatic nerve; sn, spinal nerves; st, stomach

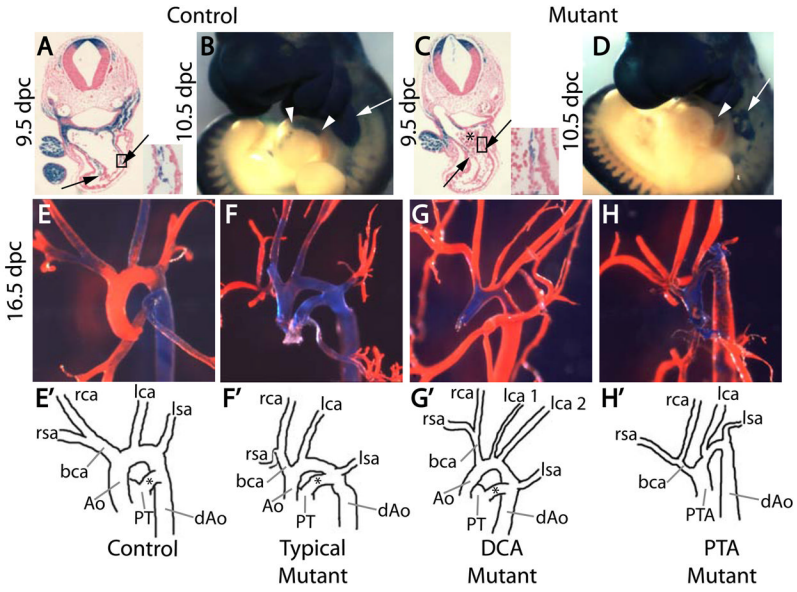


**Figure 5. Deletion of Foxd3 in the NC has subtle infrequent effects on heart development**

**A-B.** At 9.5 dpc, a section through a lineage labeled control embryo shows NC entering the developing heart (arrows). Location of the inset is indicated by the black box. In a control embryo at 10.5 dpc, NC are located in PA 3 and 4 (arrow) and have migrated into the heart (between arrowheads). **C**–**D.** At 9.5 dpc, a section through a mutant embryo shows NC entering the developing heart (arrows). Asterisk marks blood inside the heart. In a mutant embryo at 10.5 dpc, very few NC are migrating into the heart (arrowhead) and very little NC is detected in PA 3 and 4 (arrow). **E**–**H.** Corrosion casts of 16.5 dpc cardiac outflow tract and associated vessels. **E**′–**H**′ show corresponding traces. The majority of mutants (13 of 17) are indistinguishable from controls (E–F). A few mutants had a duplicated left carotid artery (3 of 17) (G) and one mutant had a PTA (H).

Ao, aorta; bca, brachiocephalic artery; dAo, dorsal aorta; DCA, duplicated carotid artery, lca, left carotid; lsa, left subclavian artery; PT, pulmonary trunk; PTA, persistent truncus arteriosus; rca, right carotid artery; rsc, right subclavian artery; * denotes the ductus arteriosus.

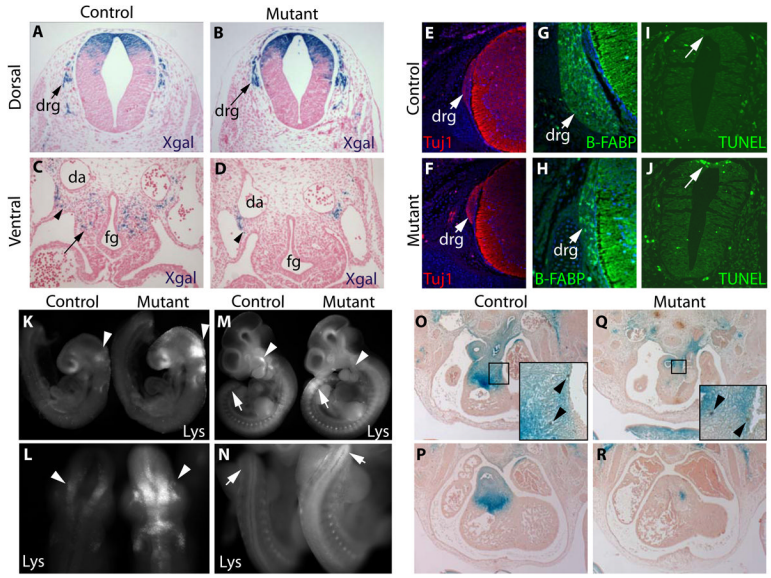


**Figure 6. Cell migration, survival and proliferation effects**

**A-B.** Sections through lineage labeled 9.5 dpc control and mutant embryos show NC have migrated ventrally to form the DRG. Samples stained as in Figure 5. **C–D.** A more ventral view of the same region pictured in A and B shows NC populating the foregut in the control embryo (arrow) but halting migration near the dorsal aorta in the mutant (arrowhead). **E–H.** Control and mutant DRG contain differentiated neurons and glia at 14.5 dpc as indicated by Tuj1 and B-FABP/FABP7 expression. **I–J.** Marked changes in cell death occur in the dorsal spinal cord of 9.5 dpc mutant embryos. **K–N.** Whole 9.0 dpc embryos incubated in LysoTracker Red to indicate dying cells. Note pronounced cell death in the mutant hindbrain and migrating NC (arrowheads). At 10.5 dpc (M-N) the mutant has fewer apoptotic cells in the distal region of the PAs (arrowheads), but increased apoptotic cells in the tail (arrows). The overall loss of PA tissue is apparent. **O–P.** Matched sections from control and mutant rostral (O and Q) and caudal (P and R) outflow tracts with lineage label (blue) and pH3 immunostaining (brown) showing reduced NC in the mutant outflow tract. The box indicates area of the inset.

## Table 1

**A. Genotypes of offspring and embryos from representative *Foxd3*$^{flox/+}$ × *Foxd3*$^{+/-}$; *Wnt1-Cre* crosses.**

| | 1 | 2 | 3 | 4 | 5 | 6 | |
|---|---|---|---|---|---|---|---|
| **Age** | ***Foxd3*$^{flox/-}$; *Wnt1-Cre* (mutants)** | ***Foxd3*$^{flox/+}$; *Wnt1-Cre*** | ***Foxd3*$^{+/+}$ or *Foxd3*$^{+/-}$; *Wnt1-Cre*** | ***Foxd3*$^{flox/-}$** | **Foxd3$^{flox/+}$** | ***Foxd3*$^{+/+}$ *Foxd3*$^{+/-}$** | **Total n** |
| Expected frequency | 12.5% | 12.5% | 25% | 12.5% | 12.5% | 25% | |
| 8.5 dpc | 2 (18%) | 0 | 4 (36%) | 0 | 1 (9%) | 4 (36%) | 11 |
| 9.5 dpc | 16 (12%) | 17 (13%) | 40 (30%) | 11 (8%) | 21 (16%) | 30 (22%) | 135 |
| 10.5 dpc | 1 (6%) | 3 (19%) | 4 (25%) | 3 (19%) | 2 (12%) | 3 (19%) | 16 |
| 12.5 dpc | 1 (8%) | 1 (8%) | 3 (25%) | 3 (25%) | 2 (17%) | 2 (17%) | 12 |
| Newborn | 1* (3%) | 9 (24%) | 7 (18%) | 6 (16%) | 4 (11%) | 11 (29%) | 38 |
| Total | 21 (10%) | 30 (14%) | 58 (27%) | 23 (11%) | 30 (14%) | 50 (24%) | 174 |

**B. Genotypes of embryos from representative *Foxd3*$^{flox/flox}$ × *Foxd3*$^{+/-}$; *Wnt1-Cre* crosses.**

| | 1 | 2 | 3 | 4 | |
|---|---|---|---|---|---|
| **Age** | ***Foxd3*$^{flox/-}$; *Wnt1-Cre* (mutants)** | ***Foxd3*$^{flox/+}$; *Wnt1-Cre*** | ***Foxd3*$^{flox/-}$** | ***Foxd3*$^{flox/+}$** | **Total n** |
| **Expected frequency** | **25%** | **25%** | **25%** | **25%** | |
| 9.5 dpc | 19 (20%) | 27 (29%) | 23 (25%) | 24 (26%) | 93 |
| 16.5 dpc | 4 (33%) | 2 (17%) | 3 (25%) | 3 (25%) | 12 |
| Total | 23 (22%) | 29 (28%) | 26 (25%) | 27 (26%) | 105 |

* 1 newborn pup was found dead in the third litter (pictured in Fig. 2a).

Percentages are rounded to the nearest whole number.